Biogeosciences, 9, 1253–1265, 2012
www.biogeosciences.net/9/1253/2012/
doi:10.5194/bg-9-1253-2012

Biogeosciences

^{210}Pb-^{226}Ra chronology reveals rapid growth rate of *Madrepora oculata* and *Lophelia pertusa* on world's largest cold-water coral reef

P. Sabatier[1,2], J.-L. Reyss[3], J. M. Hall-Spencer[4], C. Colin[2], N. Frank[3], N. Tisnérat-Laborde[3], L. Bordier[3], and E. Douville[3]

[1]Université de Savoie, UMR5204, CNRS – Laboratoire Environnement Dynamiques et Territoire de Montagne, 73376 Le Bourget du Lac, France
[2]Université Paris-Sud 11, UMR8148, CNRS/INSU – Laboratoire des Interactions et de la Dynamique des Environnements de Surface, 91405 Orsay, France
[3]Laboratoire des Sciences du Climat et de l'Environnement, UMR8212, UVSQ/CNRS/CEA, Domaine du CNRS, 91198 Gif/Yvette, France
[4]Marine Biology and Ecology Research Centre, School of Marine Science and Engineering, University of Plymouth, Plymouth, PL4 8AA, UK

Correspondence to: P. Sabatier (pierre.sabatier@univ-savoie.fr)

Received: 6 December 2011 – Published in Biogeosciences Discuss.: 21 December 2011
Revised: 2 March 2012 – Accepted: 7 March 2012 – Published: 30 March 2012

Abstract. Here we show the use of the ^{210}Pb-^{226}Ra excess method to determine the growth rate of two corals from the world's largest known cold-water coral reef, Røst Reef, north of the Arctic circle off Norway. Colonies of each of the two species that build the reef, *Lophelia pertusa* and *Madrepora oculata*, were collected alive at 350 m depth using a submersible. Pb and Ra isotopes were measured along the major growth axis of both specimens using low level alpha and gamma spectrometry and trace element compositions were studied. ^{210}Pb and ^{226}Ra differ in the way they are incorporated into coral skeletons. Hence, to assess growth rates, we considered the exponential decrease of initially incorporated ^{210}Pb, as well as the increase in ^{210}Pb from the decay of ^{226}Ra and contamination with ^{210}Pb associated with Mn-Fe coatings that we were unable to remove completely from the oldest parts of the skeletons.

^{226}Ra activity was similar in both coral species, so, assuming constant uptake of ^{210}Pb through time, we used the ^{210}Pb-^{226}Ra chronology to calculate growth rates. The 45.5 cm long branch of *M. oculata* was 31 yr with an average linear growth rate of 14.4 ± 1.1 mm yr^{-1} (2.6 polyps per year). Despite cleaning, a correction for Mn-Fe oxide contamination was required for the oldest part of the colony; this correction corroborated our radiocarbon date of 40 yr and a mean growth rate of 2 polyps yr^{-1}. This rate is similar to the one obtained in aquarium experiments under optimal growth conditions.

For the 80 cm-long *L. pertusa* colony, metal-oxide contamination remained in both the middle and basal part of the coral skeleton despite cleaning, inhibiting similar age and growth rate estimates. The youngest part of the colony was free of metal oxides and this 15 cm section had an estimated a growth rate of 8 mm yr^{-1}, with high uncertainty (~1 polyp every two to three years). We are less certain of this ^{210}Pb growth rate estimate which is within the lowermost ranges of previous growth rate estimates.

We show that ^{210}Pb-^{226}Ra dating can be successfully applied to determine the age and growth rate of framework-forming cold-water corals if Mn-Fe oxide deposits can be removed. Where metal oxides can be removed, large *M. oculata* and *L. pertusa* skeletons provide archives for studies of intermediate water masses with an up to annual time resolution and spanning over many decades.

1 Introduction

Cold-water corals have been known since the 18th century, but much less is known about their ecology and growth patterns compared to their shallow water counterparts (Roberts et al., 2009). Recently, advances in acoustic survey techniques and more widespread use of ROVs and submersibles have allowed detailed in situ studies of cold-water coral habitats showing their ecological importance for a diverse range of invertebrates and fish (Roberts et al., 2009; Söffker et

al., 2011). Cold-water coral reefs are threatened by damaging fishing practices worldwide (Hall-Spencer et al., 2009; Clark et al., 2010). In addition, increasing anthropogenic CO_2 emissions are rapidly lowering the aragonite saturation state of seawater (Guinotte et al., 2006; Tittensor et al., 2010), which combined with ocean warming can adversely affect temperate coral growth (Rodolfo-Metalpa et al., 2011). Knowledge of cold-water coral reefs growth is central to inform policy makers who decide about fishing impacts and reef management in the face of ocean acidification and ocean warming.

Cold water corals occur in all ocean basins, typically within temperatures of 4–12 °C in areas with strong near-bottom currents, enhanced labile organic matter fluxes, low sedimentation rates and availability of hard substrata to colonize (Roberts et al., 2009). The aragonitic skeletons of cold water scleractinian corals are being used as archives to trace past climate and ocean circulation patterns (Adkins et al., 1998; Magini et al., 1998; Heikoop et al., 2002; Thresher et al., 2004; Frank et al., 2005; van de Flierdt et al., 2006; Colin et al., 2010; Copard et al., 2010). The skeletons are usually dated using ^{230}Th/U and ^{14}C (Adkins et al., 1998; Mangini et al., 1998; Cheng et al., 2000; Frank et al., 2004, 2009) and the aragonite can incorporate numerous tracers of water-mass provenance, state of ventilation and surface ocean productivity. However, U-series dating and ^{14}C dating is most successful on time scales from decades to thousands of years; reconstructing the individual growth rate of a single organisms can be achieved through a large amount of mass spectrometric analyses at very high analytical precision. Alternatively, an age model for recent corals can be established using ^{210}Pb-^{226}Ra methodology (Moore and Krishnaswami, 1972; Dodge and Thomson, 1974; Druffel et al., 1990; Andrews et al., 2002, 2009; Adkins et al., 2004). This method uses the radioactive decay of ^{210}Pb (half life of 22.3 yr) in excess to its parent, ^{226}Ra, to determine mean growth rates. Other techniques, such as counting growth rings (Grigg, 1974) or carbon and oxygen isotopic variations (Fairbanks and Dodge, 1979) in skeletons, have been employed to estimate the age of recent coral specimens. However, for most of those species, independent in-situ observations and growth rate measurements have not been available to validate the radiometric dating technique.

^{210}Pb-^{226}Ra dating has not been previously applied to the major reef-building corals *L. pertusa* and *M. oculata*. Their complex branching and anastomizing complex colonies have proved difficult for sclerochronology (Risk et al., 2005). However, the occurrence of these species is strongly influenced by climate (Rüggeberg et al., 2008; Frank et al., 2009, 2011) and their skeletons can be used to reconstruct water mass provenance (Colin et al., 2010; Copard et al., 2010, 2011). For both species, independent growth rate estimates have been obtained from in situ observations and aquarium studies. In the North Atlantic, *L. pertusa* mean growth rate was estimated at $26 \pm 5\,\mathrm{mm\,yr^{-1}}$ by measuring the size of coral colonies observed on oil an gas plateforms (Bell and Smith, 1999; Gass and Roberts, 2006). Using the buoyant weight technique for specimens maintained in aquaria, Orejas et al. (2008) have found extension rates of 15–17 mm yr^{-1} for *L. pertusa*, and between 3 and 18 mm yr^{1} for *M. oculata*.

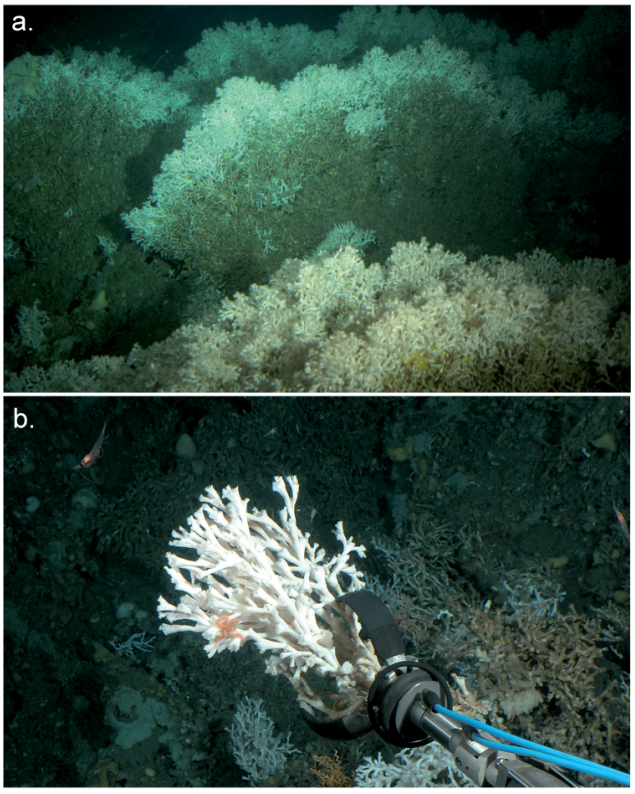

Fig. 1. Submersible dives on Røst reef in June 2007, **(a)** image taken looking down a steep wall with large *L. pertusa* buttresses extending 3–4 m out from the substratum; dead skeletons are encrusted in brown metal oxides, living parts are white (67°30′30″ N 9°25′30″ E, 340 m depth). **(b)** Coral collection from reef crest formed by orange and white *M. oculata* and *L. pertusa* colonies. Krill and copepods were abundant during sample collection (67°30′20″ N 9°24′45″ E, 300 m depth).

Here we have performed ^{210}Pb-^{226}Ra dating on two framework forming specimens from Røst reef in Norway; this is the world's largest known deep-water coral reef where the corals thrive on the continental shelf break region above the Arctic circle. There is growing concern that ocean acidification may hinder growth and encourage dissolution of this reef complex, as the effects of ocean acidification are exacerbated at high latitudes (Maier et al., 2009; Tittensor et al., 2010). Assessing the mean growth rate and polyp reproduction rate over recent decades provides a baseline against which to monitor coral growth models as aragonite saturation levels fall. This provides an independent estimate of recent mean growth rates. Here we evaluate the ^{210}Pb-^{226}Ra dating methodology to establish coral growth models that are then

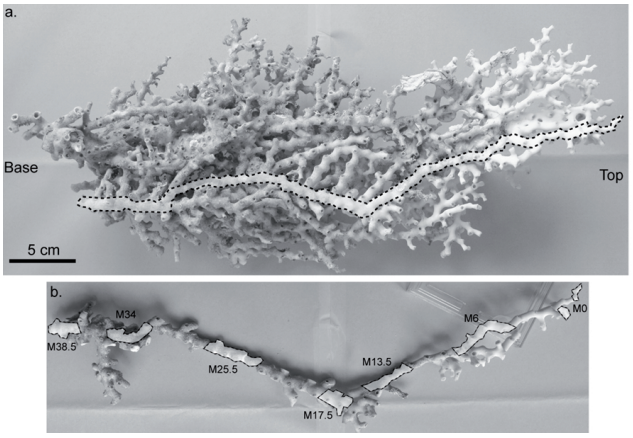

Fig. 2. Subsampling of *Madrepora oculata* specimen. **(a)** Extraction of a continuous branch along the coral, **(b)** location of samples analyzed for ^{210}Pb-^{226}Ra chronology.

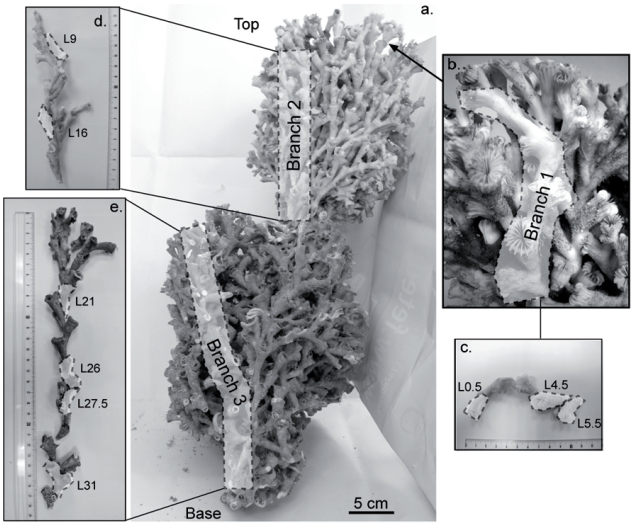

Fig. 3. **(a)** Photograph of a *Lophelia pertusa* specimen with the identification of branch 2 and 3, **(b)** location and identification of branch 1 in the upper part of the coral. Location of samples analyzed for ^{210}Pb-^{226}Ra chronology on extracted branch 1 **(c)**, branch 2 **(d)** and branch 3 **(e)**.

compared to independent growth rate estimates and polyp budding cycles. Finally, we discuss some limitations of the ^{210}Pb-^{226}Ra technique for reef forming cold water corals.

2 Coral samples and cleaning

Corals were collected from Røst Reef during the ARK-XXII/1a cruise on the RV Polarstern, using the manned submersible Jago, in June 2007 (Fig. 1). Røst Reef, discovered in May 2002, is a reef-complex 35–40 km long, up to 3 km wide situated at 300–400 m depth along a steep and rugged part of the continental shelf break off Norway (Fosså et al., 2005). We collected *L. pertusa* and *M. oculata* corals from 300–350 m depth between 67°30′ N and 67°32′ N; and 9°24′30″ E and 9°30′30″ E and the largest intact colonies were retained for geochemical analyses (Fig. 1). Fig. 1a shows an image taken from the Jago submersible dive on Røst reef (67°30′30″ N 9°25′30″ E, 340 m depth), with a large *L. pertusa* buttresses extending 3–4 m out from the substratum. This picture illustrates that dead skeletons are encrusted in brown metal oxides while living parts are white.

The *M. oculata* colony was 46 cm long and 18 cm wide and composed of hundreds of successive corallites. Samples were taken for radiometric and trace element analyses along a continuous 45.5 cm branch formed by 80 corallites (Fig. 2). This coral branch was divided perpendicularly to its growth axis into 40 samples of 2 corallites each. The *L. pertusa* was 50 cm long and 20 cm wide and again composed of hundreds of corallites. It had complex branching so three segments with a total length of 80 cm were cut out and sub-divided into 33 samples of 1 coralline each (Fig. 3).

The coral skeletons that had been exposed to seawater had been subject to post-mortem deposition of ferromanganese oxide and hydroxide coatings (Fig. 1a; see also Lomitschka and Mangini, 1999; Cheng et al., 2000). Adkins et al. (2004) showed that this surface contamination had to be removed prior to U-series dating. In our study, coral skeletons were subsampled by cutting and then cleaned following the procedure described by Copard et al. (2010). Corals polyps were cut in half and rinsed in MilliQ water to remove sediments from the external and internal surface. The inner and outer surfaces of the skeletons were polished using a diamond-bladed saw to remove surface contaminants such as ferromanganese coatings and remains of organic matter. At this stage, we avoided segments that had skeleton alteration due to boring organisms (Beuck et al., 2007). This mechanical cleaning was followed by a weak acid treatment with 0.1 N ultraclean hydrochloric acid in an ultrasonic bath, and the corals were then rinsed several times with MilliQ water. Cleaned samples were then dried at 54 °C for 2 h, crushed to powder in an agate pestle-mortar and weighed.

In addition, four Mb, Mt and Lb, Lt samples were extracted at the base and the top of the two specimens, but on different branches, M and L respectively for *M. oculata* and *L. pertusa*. Here, no cleaning was applied to analyse the bulk sample radionuclide composition including the coral's potentially contaminated surface.

3 Analytical methods

^{210}Pb, ^{226}Ra, ^{228}Ra, ^{228}Th, ^{234}Th and ^{40}K activities were analyzed on samples using well-type, germanium detectors placed at the Laboratoire Souterrain de Modane (LSM), located under 1700 m of rock. The reduction of crystal background was obtained by the selection of low-activity

materials and the suppression of cosmic radiations by placing the detectors in the LSM (Reyss et al., 1995). At the same time, the detector sensitivity allows the reduction of sample mass required for a measurement. These improvements allow measurements of both very low radioactivity levels (with background less than 0.6 counts per minute for the 30–3000 keV energy range) and small sample weights (1 g). The ^{226}Ra activities were determined using its short-lived daughters ^{214}Pb (295 keV and 352 keV peaks) and ^{214}Bi (609 keV peak), assuming secular equilibrium with ^{226}Ra. The ^{238}U activities in coral sample were determined through its ^{234}Th daughter peak (63.2 keV). ^{40}K was measured through its gamma emissions at 1460 keV, while ^{228}Th and ^{228}Ra are measured using the gamma-ray emitted by their short-lived descendants: ^{212}Pb (238 keV) and ^{208}Tl (583 keV) for ^{228}Th and ^{228}Ac (338, 911, and 970 keV) for ^{228}Ra. The ^{210}Pb (22.3 yr) activity was directly measured through its gamma emissions at 46.5 keV, but the very low activity of ^{210}Pb does not allow to us obtain an accurate estimation with uncertainties of about 30 %. Therefore, ^{210}Pb detection was accomplished by alpha-spectrometry determination of its daughter ^{210}Po (138 d). The extraction was made 2 yr after the collection of the sample to ensure secular equilibrium with ^{210}Pb. For alpha spectrometric measurements, ∼1 g of cleaned coral of dissolved in 15 ml of 2 N HCl and 1 ml of 2 % $HClO_4$ and spiked with 1 ml of an 11.8 mBq g^{-1} ^{208}Po solution. The solution was evaporated and then bathed in 1 ml of 2 % $HClO_4$ to fully remove organic matter. The residue was dissolved in 8 N HCl and diluted with Milli-Q water to obtain a 30 ml solution of 0.5 N HCl. The solution was auto-plated onto silver disks at ∼75 °C for 4 h in the presence of ascorbic acid, following the procedure describe by Flynn (1968). Alpha-spectrometry was performed using grid chamber detectors at the Laboratoire du Climat et de l'Environnement (LSCE) at Gif/Yvette (France). Uncertainties for ^{210}Pb analyses are given as 1σ uncertainty of counting statistics of samples and blanks. Mn concentrations of corals were analysed on cleaned and dissolved coral fragments using a quadruple ICP-MS (Inductively Coupled Plasma Mass Spectrometry) Xseries$^{II(Thermo)}$ following the bracketing protocol described by Copard et al. (2010). Samples and standard solutions were systematically adjusted to 100 ppm Ca through dilution. Instrumental calibration based on the standard addition method was achieved using a mono-elementary standard solution. Internal reproducibility for Mn on the Japanese coral *Porites* sp. (JCp-1) standard (100 ppm Ca) was about 5 % (2σ).

Accelerator Mass Spectrometry (AMS) radiocarbon analyses were conducted on five sample aliquots of the *M. oculata* branch of about 10–20 mg size following the procedure published previously (Frank et al., 2004). Samples were converted to CO_2 in a semi-automated carbonate vacuum line (Tisnérat-Laborde et al., 2001), reduced to graphite using hydrogen in the presence of iron powder (Arnold et al. 1989), and measured by the AMS-LMC14 (Laboratoire de Mesure du Carbon 14) Artemis accelerator facility (Cottereau et al., 2007). They are expressed as pMC normalised to a δ^{13}C of −25 ‰ relative to the Vienna Pee Dee Belemnite (PDB) international standard according to Stuiver and Polach (1977).

4 ^{210}Pb-^{226}Ra dating method

Since Goldberg (1963) first established a method based on ^{210}Pb chronology, this procedure has provided a very useful tool for dating environmental archives, recently including cold-water coral (Adkins et al., 2004). ^{210}Pb precipitates from the atmosphere through ^{222}Rn decay and is scavenged from the surface ocean to deep and intermediate waters where it accumulates on the surface of sediments and corals. In each of our coral samples, the ^{210}Pb excess activities were calculated by subtracting the ^{226}Ra activity, derived from the detritic component, from the total (^{210}Pb) activity. In the simplest model, the initial excess of ^{210}Pb activity (^{210}Pb$_{ex}$) is assumed constant and thus (^{210}Pb$_{ex}$) at any time is given by the radioactive decay law (Appleby and Oldfield, 1992). Throughout this paper, parentheses denote specific activity.

$$(^{210}\mathrm{Pb}_{ex}) = (^{210}\mathrm{Pb}^{0}_{ex})e^{-\lambda_{210}t} \quad (1)$$

$$\text{with } (^{210}\mathrm{Pb}_{ex}) = (^{210}\mathrm{Pb}) - (^{226}\mathrm{Ra}) \quad (2)$$

This ^{210}Pb$_{ex}$ method was applied to determine the growth rate of biogenic carbonates such as marine mollusc shells (Cochran et al., 1981; Turekian and Cochran, 1986) and tropical as well as deep dwelling corals (Moore and Krishnaswami, 1972; Dodge and Thomson, 1974; Druffel et al., 1990; Andrews et al., 2002, 2009; Adkins et al., 2004).

Another method based on ^{210}Pb ingrowth from the ^{226}Ra allows dating of recent carbonates such as near-shore mollusc shells (Baskaran et al., 2005), fish otoliths (Fenton et al., 1991) and whale bones (Schuller et al., 2004). This ^{210}Pb ingrowth method requires either that the initial ^{210}Pb incorporated is negligible compared to the radiogenic ^{210}Pb produced by the decay of ^{226}Ra, or that its initial activity can be estimated. Moreover, the use of this method supposes that the carbonate behaves as a closed system (Baskaran et al., 2005). Thus, ^{210}Pb ingrowth with time is described by the following radioactive decay equation:

$$(^{210}\mathrm{Pb}) = \frac{\lambda_{210}}{\lambda_{210}-\lambda_{226}}(^{226}\mathrm{Ra})\left[1-e^{-(\lambda_{210}-\lambda_{226})t}\right] \quad (3)$$

Since ^{226}Ra has a much longer half-life (1600 yr) than ^{210}Pb (22.3 yr) (or $\lambda_{Pb} \ll \lambda_{Ra}$), this equation is usually written in its simplified form:

$$(^{210}\mathrm{Pb}) = (^{226}\mathrm{Ra})\left[1-e^{-\lambda_{210}t}\right] \quad (4)$$

To date young biogenic carbonates (otoliths, bivalve shells and coral), the use of excess (Eq. 1) or ingrowth (Eq. 4) method mostly depends on the ratio (^{210}Pb/^{226}Ra) of the water in which the organism forms and on the pathways (internal or external organs) by which ions are incorporated into the carbonate (e.g. Schmidt and Cochran, 2010).

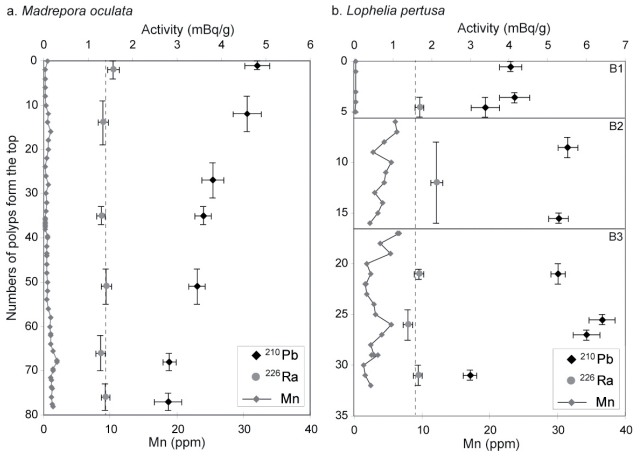

Fig. 4. ^{210}Pb activities (black dots), ^{226}Ra activities (grey dots) and Mn content (grey curve) from mechanically and chemically cleaned polyps of *Madrepora oculata* **(a)** and *Lophelia pertusa* **(b)** specimens. Dotted line displays the mean activity of ^{226}Ra. Horizontal dotted lines represent the limit of the three sampled branches of *Lophelia pertusa* (B1, B2, and B3).

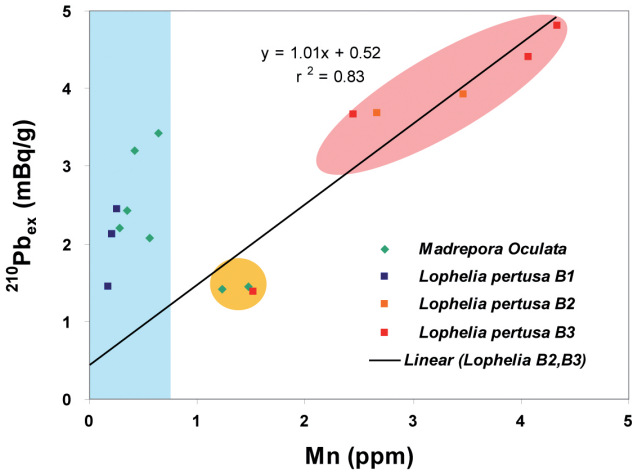

Fig. 5. ^{210}Pb excess versus Mn concentrations for the two *Madrepora oculata* and *Lophelia pertusa* specimens studied here. This graph reveals a marked link between the presence of Mn-oxydes and the level of ^{210}Pb excess for the older parts of each coral fragment. Such an effect strongly limits the use of the ^{210}Pb-^{226}Ra method for older Mn-rich deep-sea corals. Red, orange and blue areas represent respectively highly, moderately and slightly Mn-contaminated coral samples.

5 Results

^{210}Pb in "uncleaned" coral skeletons with obvious metal oxide deposits had very large ^{210}Pb activity (72.2 and 161.8 mBq g^{-1}) in the oldest parts of the colonies (M_b and L_b), whereas apical samples (M_t, L_t) had far less ^{210}Pb (7.8 and 5.1 mBq g^{-1}, see Tables 1 and 2). Thus, the ^{210}Pb composition of uncleaned samples is clearly opposite to the expectation that ^{210}Pb is constantly precipitated as the organism grows and decays with increasing age of the skeleton. The base of both corals, however, is more affected by post-depositional ferromanganese oxide coatings as dead corallites are no longer kept clean by the mucus that protects the skeleton around living polyps (Fig. 1a). In contrast ^{226}Ra activities were almost constant for all the *M. oculata* samples (clean or not) and for *L. pertusa* the uncleaned coral had a ^{226}Ra activity slightly higher at the base.

Rigorously cleaned samples from both coral specimens displayed by far weaker ^{210}Pb excess activities (<6 mBq g^{-1}) and more importantly reveal a decrease of ^{210}Pb activities from the top to the base (see Fig. 4). In addition, the ^{226}Ra activities were very similar and can be considered constant within uncertainty with mean values of 1.37 ± 0.05 and 1.60 ± 0.06 mBq g^{-1} for *M. oculata* and *L. pertusa*, respectively. Solely one sample (polyp 12.5) within the *L. pertusa* colony had a minor increase from this mean value (see Fig. 4b). Mn concentrations were also measured on each cleaned sample to indicate the presence of residual metal oxide coatings that could alter ^{210}Pb profiles. Mn concentrations of *M. oculata* (Fig. 4a) are between 0.2 and 2 ppm (5 % of uncertainty), with lowest values at the top (live) polyps and highest values at the base (fossil) polyps. Similarly apical *L. pertusa* corallites had low Mn contents (around 0.2 ppm) (Fig. 4b), but much higher values (between 1.4 and 6.6 ppm) were measured for the middle and basal branches 2 and 3, revealing residual metal oxide contamination that was not removed by cleaning.

^{210}Pb activities analyzed along the growth axis of *L. pertusa* vary between 6.40 ± 0.34 mBq g^{-1} and 2.99 ± 0.17 mBq g^{-1} and do not reveal a clear decreasing trend along the growth axis as expected from ^{210}Pb decay. However, all (^{210}Pb/^{226}Ra) activity ratios along the coral specimen clearly exceeded secular equilibrium indicating that this *L. pertusa* is probably younger than 100 yr. But, the highest ^{210}Pb activities within the middle and basal branches coincide with high residual Mn concentrations and one may thus suspect that both branches contain a significant amount of post-depositional ^{210}Pb as observed far more importantly in the uncleaned samples. For the oldest part of the two last branches of *L. pertusa*, a correlation between high Mn content an high ^{210}Pb excess activity was found ($r^2 = 0.83$, $n = 6$) (Fig. 5), whereas such a correlation was absent for the youngest samples of this specimen (blue area). Thus, ^{210}Pb activities in this specimen probably do not reflect the subsequent incorporation and decay thought.

Along the growth axis of *M. oculata* ^{210}Pb activities decrease systematically from 4.80 ± 0.28 mBq g^{-1} (top) to 2.80 ± 0.30 mBq g^{-1} (base). The length of the coral is expressed here in number of polyps from the top. All (^{210}Pb/^{226}Ra) activity ratios along the coral specimen are once more clearly above secular equilibrium indicating that

Table 1. Radiometric data from the *Madrepora oculata* specimen, activity was determined as milli-Becquerel per gram ($mBq\,g^{-1}$) with standard deviation at 1σ. In bold, data obtained by gamma spectrometry with activities of ^{210}Pb, ^{226}Ra, ^{238}U, ^{228}Th, ^{228}Ra and ^{40}K. In regular, ^{210}Pb activities obtained by alpha spectrometry. Mn contents were expressed in ppm.

Polyps	Mass (g)	^{210}Pb ($mBq\,g^{-1}$)	^{226}Ra ($mBq\,g^{-1}$)	^{238}U ($mBq\,g^{-1}$)	^{228}Th ($mBq\,g^{-1}$)	^{228}Ra ($mBq\,g^{-1}$)	^{40}K ($mBq\,g^{-1}$)	Mn (ppm)
2	**1.453**	**3.8 ± 1.1**	**1.57 ± 0.13**	**48.3 ± 2.7**	**0.37 ± 0.05**	**0.09 ± 0.03**	**0.48 ± 0.07**	
1	0.971	4.8 ± 0.28						0.64
14	**1.97**	**4.4 ± 1**	**1.34 ± 0.11**	**41 ± 2**	**0.28 ± 0.05**	/	**0.25 ± 0.03**	
12	0.936	4.58 ± 0.31						0.42
27	0.995	3.81 ± 0.24						0.35
35	**2.15**	**4.1 ± 0.8**	**1.29 ± 0.1**	**37 ± 2**	**0.25 ± 0.04**	/	**0.22 ± 0.03**	
35	1.135	3.59 ± 0.19						0.28
51	**2.041**	**4.5 ± 0.9**	**1.41 ± 0.11**	**42 ± 2**	/	/	**0.22 ± 0.03**	
51	0.987	3.45 ± 0.18						0.55
66	**2.13**	**3.9 ± 0.9**	**1.28 ± 0.1**	**41 ± 2**	**0.26 ± 0.04**	**0.2 ± 0.08**	**0.23 ± 0.03**	
68	0.994	2.83 ± 0.15						1.47
76	**2.21**	**2.9 ± 0.8**	**1.39 ± 0.1**	**38 ± 2**	**0.31 ± 0.05**	**0.19 ± 0.08**	**0.13 ± 0.03**	
77	0.987	2.8 ± 0.3						1.23
Mt	**1.72**	**7.8 ± 1.0**	**1.93 ± 0.10**	**47.2 ± 2**	**0.22 ± 0.02**	**0.26 ± 0.06**	**0.35 ± 0.04**	
Mb	**2.07**	**72.2 ± 4.4**	**1.96 ± 0.21**	**48.6 ± 4**	**2.09 ± 0.2**	**0.19 ± 0.12**	**0.47 ± 0.09**	

Table 2. Radiometric data from the *Lophelia pertusa* specimen, activity was determined as milli-Becquerel per gram ($mBq\,g^{-1}$) with standard deviation at 1σ. In bold, data obtained by gamma spectrometry with activities of ^{210}Pb, ^{226}Ra, ^{238}U, ^{228}Th, ^{228}Ra and ^{40}K. In regular, ^{210}Pb activities obtained by alpha spectrometry. Some samples are below the limit of detection (/). Mn contents were expressed in ppm.

Polyps	Mass (g)	^{210}Pb ($mBq\,g^{-1}$)	^{226}Ra ($mBq\,g^{-1}$)	^{238}U($mBq\,g^{-1}$)	^{228}Th ($mBq\,g^{-1}$)	^{228}Ra ($mBq\,g^{-1}$)	^{40}K ($mBq\,g^{-1}$)	Mn (ppm)
0.5	0.71	4.04 ± 0.28						0.25
5	**2.045**	**2.9 ± 0.9**	**1.69 ± 0.11**	**33 ± 2**	**0.5 ± 0.05**	**0.09 ± 0.03**	**0.53 ± 0.07**	
4.5	0.87	3.72 ± 0.34						0.21
5.5	1.177	3.04 ± 0.34						0.17
12.5	**1.02**	**5.9 ± 1.4**	**2.13 ± 0.16**	**37 ± 3**	**2.7 ± 0.17**	**0.5 ± 0.13**	**0.53 ± 0.07**	
9	0.51	5.52 ± 0.26						3.46
16	0.5	5.28 ± 0.25						2.66
21	**2.12**	**2.3 ± 1**	**1.68 ± 0.12**	**36 ± 2**	**0.39 ± 0.05**	**0.25 ± 0.07**	**0.35 ± 0.05**	
20.5	1.1	5.27 ± 0.18						2.45
26.5	**1.3**	**5.6 ± 1.2**	**1.39 ± 0.12**	**38.6 ± 2.5**	**1.31 ± 0.1**	**0.09 ± 0.04**	**0.42 ± 0.05**	
26	0.68	6.4 ± 0.34						4.34
27.5	0.62	6 ± 0.34						4.08
31	**1.74**	**3.9 ± 0.9**	**1.65 ± 0.11**	**36 ± 2**	**0.05 ± 1**	/	**0.39 ± 0.05**	
31	1.74	2.99 ± 0.17						1.52
Lt	**1.79**	**5.1 ± 1.3**	**1.89 ± 0.16**	**35 ± 2**	**0.27 ± 0.06**	**0.25 ± 0.12**	**0.60 ± 0.01**	
Lbc	**1.19**	**3 ± 1.8**	**1.63 ± 0.18**	**36 ± 3**	/	/	/	
Lb	**4.68**	**161.8 ± 2.1**	**2.95 ± 0.09**	**36 ± 1**	**2.37 ± 0.07**	**0.71 ± 0.1**	**1.40 ± 0.10**	

the alive *M. oculata* sampled is again most likely less than 100 yr old. So (^{210}Pb) data obtained by alpha spectrometry can be used to establish an accurate age model on this deep-sea coral samples. However, in Fig. 5 the two oldest samples from *M. oculata* specimen were also altered by this Mn contamination (orange area).

6 Discussion

6.1 Radionuclide incorporation and implication for ^{210}Pb-^{226}Ra chronology

From ^{226}Ra and ^{210}Pb values described above, two main observations can be made. First, rigorous cleaning is mandatory to eliminate ^{210}Pb added to its surface after the skeleton has formed, whereas this cleaning was apparently not important for ^{226}Ra, confirming previous studies on solitary coral species such as *D. dianthus* (Adkins et al., 2004). Second, ^{210}Pb and ^{226}Ra are not incorporated into the coral skeletons

in the same way, reflecting the different chemical behavior of radium and lead in the marine environment (Krishnaswami and Cochran, 2008). Lead and its isotopes are readily scavenged onto particles in the water column and have a short oceanic residence time (1 yr in the surface and 30–100 yr in deeper ocean, Cochran et al., 1990) while radium is soluble in seawater and is thus not scavenged onto particle surfaces. ^{226}Ra in seawater mainly comes from diffusion from deep-sea sediments into the overlying bottom water (van Beek and Reyss, 2001). ^{210}Pb inputs to the ocean include depositions from the atmospheric, where it is produced from ^{222}Rn decay. in situ production by the decay of dissolved ^{226}Ra in seawater and the river-runoff flux of unsupported ^{210}Pb (Appleby and Oldfield, 1992). ^{226}Ra is lattice-bound and not adsorbed within the intercrystaline spaces of carbonate (Berkman and Ku, 1998) thus; ^{226}Ra is incorporated into carbonate in proportion to their ratio to calcium in seawater (D_{Ra}). In contrast, the geochemical behavior of ^{210}Pb in the ocean allows for two incorporation pathways. First, lead can be scavenged onto the coral surface where it is trapped during formation of further crystal lattice. Second, ^{210}Pb can be directly incorporated into the crystal lattice from the dissolved state of seawater. Both ^{210}Pb contributions originate from seawater which we refer to as allochtonous (^{210}Pb$_{\mathrm{all}}$). The live coral polyps keep their skeletons free from sediments and parasites with mucus but older parts of the dead skeleton are exposed to seawater where authigenic ferromanganese oxyhydroxide precipitates with associated ^{210}Pb coat onto the skeleton surface (^{210}Pb$_{\mathrm{auth}}$). This additional ^{210}Pb increases depending on the time of exposure of the coral at the seawater sediment interface. Whatever the incorporation mode is, we can define a ^{210}Pb partition coefficient (D_{Pb}) for the first phase (before the death of the polyp). Therefore, the (^{210}Pb$_{\mathrm{all}}$/^{226}Ra) incorporated in deep-sea coral depends on the respective elemental partition coefficient for lead and radium, and the (^{210}Pb)/(^{226}Ra) ratio of the seawater in which the coral grows (Schmidt and Cochran, 2010):

$$\left(\frac{^{210}\mathrm{Pb}}{^{226}\mathrm{Ra}}\right)_{\mathrm{Carbonate}} = \left(\frac{D_{\mathrm{Pb}}}{D_{\mathrm{Ra}}}\right)\left(\frac{^{210}\mathrm{Pb}}{^{226}\mathrm{Ra}}\right)_{\mathrm{Water}} \quad (5)$$

For scleractinian corals ^{226}Ra is incorporated from seawater and is thus not at secular equilibrium with its radioactive daughter ^{210}Pb. Hence, when (^{210}Pb$_{\mathrm{all}}$/^{226}Ra) ratio exceeds 1, we can not applied the classical excess method, with initial ^{226}Ra at secular equilibrium with ^{210}Pb. Therefore, to describe the temporal variation of ^{210}Pb (^{210}Pb$_{\mathrm{t}}$), we have to take into account either the decrease of (^{210}Pb$_{\mathrm{all}}$) initially incorporated to the skeleton and the radiogenic ^{210}Pb induced by the ingrowth from ^{226}Ra (^{210}Pb$_{\mathrm{rad}}$), as suggested by Dodge and Thomson (1974), (Fig. 6):

$$(^{210}\mathrm{Pb_t}) = (^{210}\mathrm{Pb_{rad}}) + (^{210}\mathrm{Pb_{all}})$$
$$(^{210}\mathrm{Pb_t}) = \underbrace{(^{226}\mathrm{Ra_t})\left[1-e^{-\lambda_{210}t}\right]}_{\text{Ingrowth}} + \underbrace{(^{210}\mathrm{Pb_0})e^{-\lambda_{210}t}}_{\text{Decrease}}$$

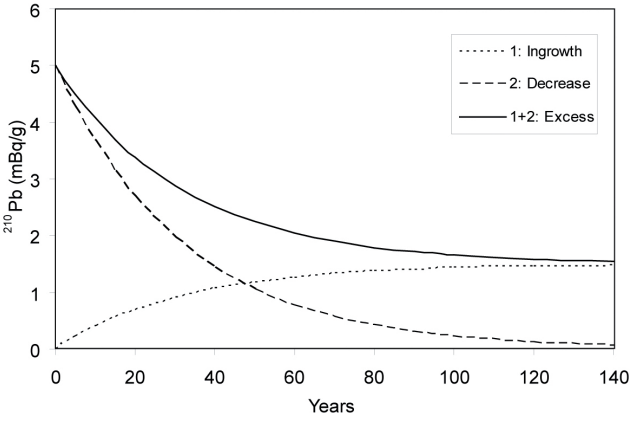

Fig. 6. Theoretical evolution of ^{210}Pb activity as a function of time for the decrease (1), ingrowth (2) and excess model (1 + 2). The excess model is the sum of decrease and ingrowth patterns.

$$(^{210}\mathrm{Pb_t}) = (^{226}\mathrm{Ra_t}) + \left(^{210}\mathrm{Pb_0} - ^{226}\mathrm{Ra_t}\right)e^{-\lambda_{210}t} \quad (6)$$

If the studied system was closed and if initial ^{210}Pb (^{210}Pb$_0$) is further assumed constant, this equation allows us to date any young carbonate using the ^{210}Pb-^{226}Ra chronology, whatever the incorporation mode of these radioelements is. Therefore, the growth rate (V) was defined by the best fit of the ^{210}Pb data by the Eq. (6), with $V = z/t$, whereas z is the distance from the base of the coral (express in mm or number of polyps). If we assume that (^{226}Ra$_{\mathrm{t}}$) is constant through time, Eq. (6) can be simplified:

$$\left(^{210}\mathrm{Pb} - ^{226}\mathrm{Ra}\right)_{\mathrm{t}} = \left(^{210}\mathrm{Pb} - ^{226}\mathrm{Ra}\right)_0 \times e^{-\lambda_{210}t} \quad (7)$$

Knowing Eq. (2), this last Eq. (7) can be described by the excess model (Eq. 1) and the growth rate of the CWC can be estimated through the following equation:

$$\ln\left(^{210}\mathrm{Pb}^{t}_{\mathrm{ex}}\right) = \ln\left(^{210}\mathrm{Pb}^{0}_{\mathrm{ex}}\right) - \lambda_{210} \times \frac{z}{V} \quad (8)$$

6.2 Estimated coral growth rates

The excess of (^{210}Pb) data (Fig. 7) displays a well-constrained slope for the *M. oculata* specimen providing evidence that the uptake of initial (^{210}Pb$_{\mathrm{ex}}$) occurs at a nearly constant rate. The low Mn concentrations (Fig. 4) associated with the well-constrained slope (Fig. 7) apparently indicate that the cleaning procedure applied here successfully removed authigenic radionuclides from the skeleton surface. The exponential slope for ^{210}Pb$_{\mathrm{ex}}$ corresponds to a linear growth rate of 2.58 ± 0.19 polyp yr^{-1} or 14.4 ± 1.1 mm yr^{-1}, using Eq. (8). This growth rate estimate yields a basal age of 31 ± 3 yr (1σ) for this 45 cm-long specimen of *M. oculata*. To test the simplification of constant flux of (^{226}Ra) on growth rate estimation, we used Eq. (6) instead of 8 to determine the age of the coral (using variable flux of (^{226}Ra),

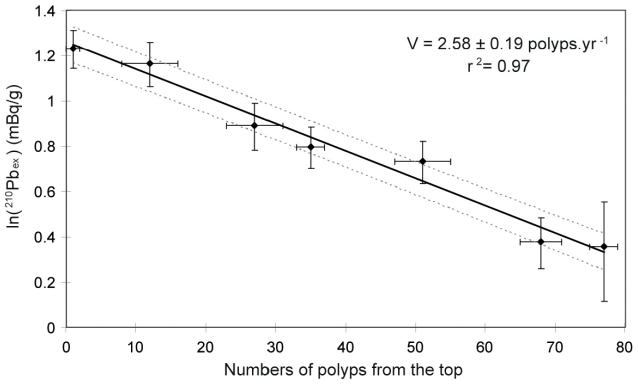

Fig. 7. ln-transformation of ^{210}Pb excess relative to the number of polyps from the top of the *Madrepora oculata* specimen. The slope of this linear regression revealed a linear growth rate of 2.58 ± 0.19 polyp yr^{-1}.

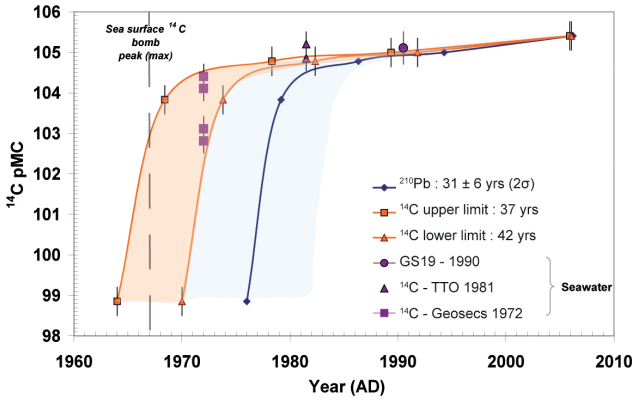

Fig. 8. Age model comparison for the *Madrepora oculata* specimen. Coral ^{14}C measurements expressed as pMC compared to available seawater ^{14}C data of dissolved inorganic carbon (see text GEOSECS, TTO and Norwegian research cruise) allow us to identify the bomb ^{14}C peak with an age for the base of between 37 and 43 yr. This estimation is in agreement at 2σ with that of ^{210}Pb-^{226}Ra method. The dashed line indicates the year of sea surface ^{14}C bomb maximum.

see Table 1) and we get the same results within uncertainties. Thus the constant flux of (^{226}Ra) assumption does not influence growth rate estimation. Moreover, with the presently available and limited data (7 measures of (^{210}Pb) regularly distributed along the branch), there is no indication of a growth interruption for this coral specimen, as no significant offset is observed between each data point (Andrews et al., 2009). To validate this age model, five independent ^{14}C analyses were performed along the *M. oculata* specimen (Table 3). They show an increase of ^{14}C data between the base and the top of the coral from 99.1 pMC to 105.6 pMC. This increase indicates that the coral recorded a part of the ^{14}C nuclear bomb produced during the era of atmospheric testing. The pre-bomb value of intermediate waters in 1950 can be estimated lower than 93 pMC if we consider that Δ^{14}C of intermediate waters are still around -70 ‰ as suggested by previous studies (Frank et al., 2004; Sherwood et al., 2008). Therefore, we can consider that *M. oculata* coral is less than 60 yr old. In order to better constrain the age scale, we compared these ^{14}C data with ^{14}C data of the dissolved inorganic carbon in seawater which are collected nearby the location of the coral during different oceanographic cruise; GEOSECS (1972, Ostlund et al., 1974), TTO cruise (1981, Broecker et al., 1985) and Norwegian research cruise (1990, Nydal et al., 1992). The ^{14}C comparison yields an age estimate between 37 and 43 yr for this specimen (Fig. 8). Thus the age from bomb-^{14}C (40 ± 3 yr) corresponds to a linear growth rate of 2 polyps yr^{-1} or 11.2 cm yr^{-1}. At 2σ uncertainty levels, bomb-^{14}C and ^{210}Pb-^{226}Ra age estimates are almost identical. The slightly younger age estimate obtained from ^{210}Pb$_{ex}$ may reflect the progressive increase of Mn contamination towards the base of the organism leading to an overestimation of ^{210}Pb$_{ex}$ values at the coral's base (Fig. 7), mainly for the two last samples identified as Mn contaminated in the Fig. 5.

In contrast, the more complex *L. pertusa* specimen presents high ^{228}Th activities with respect to the decay of its parent isotope ^{228}Ra. The half-life of ^{228}Th is 1.91 yr, thus for the oldest samples (>10 yr) the ^{228}Th/^{228}Ra activity ratio must be at secular equilibrium in a closed system. These ^{228}Th excess activities imply that this system was submitted to post-growth deposition of radionuclides, not removed by the cleaning, which probably affected the ^{210}Pb-^{226}Ra chronology.

Moreover, the elevated Mn contents, in particular of the older branches of specimen (B2 and B3) reveal also a high degree of residual skeleton contamination with ferromanganese oxide/hydroxide coatings that could apparently not be fully removed during the cleaning. We have no reasonable explanation for this yet as the cleaning protocol has been often applied to *L. pertusa* corals with excellent results regarding the removal of such coatings (Copard et al., 2010). However, if we exclude the most contaminated samples (grey points in Fig. 9, with high ^{228}Th activities and high Mn concentrations, especially for branch 3) it is possible to estimate a linear growth rate of 0.34 and 0.32 polyp yr^{-1} for the branches 1 and 3, respectively (Fig. 9), with a high degree of uncertainty related to the few points integrated for this growth rate estimation. These values would correspond to a growth rate of about 8 mm yr^{-1} and would provide a time of 18 yr covered by the more recent branch (B1). However, these estimations imply a different uptake of initial (^{210}Pb$_{ex}$) for both branches. Both growth rate estimates are in good agreement but as solely a few points are incorporated in the model and given the additional hypothesis of a variable initial (^{210}Pb$_{ex}$), this result does not seem very confident. Moreover, it is difficult to obtain a continuous section along this coral in relation to its growth complexity (Brooke and Young, 2009), thus this cold-water

Table 3. Radiocarbon data from the Madrepora oculata specimen and from dissolved inorganic carbon of water collected nearby the area of coral growth. In bold is noted the radiocarbon data expressed as pMC. The lower and upper limit of growth year was estimated by adjusting the data of M. oculata and those of seawater considering a linear growth.

Seawater Cruise ID	Station	Latitude	Longitude	Depth (m)	**pMC**	**err pMC**	Year	Reference
GEOSECS Atlantic	Station 19	64.2° N	5.6° W	247 349 458 558	**104.4** **104.1** **103.1** **102.8**	**0.3** **0.3** **0.3** **0.3**	1972	Oslund et al. (1974)
TTO	Station 144 Station 145	67.7° N 70.0° N	3.3° W 2.5° E	448 449	**104.9** **105.2**	**0.3** **0.3**	1981	Broecker et al. (1985)
Norwegian research vessels	GS 19	69.9° N	9.7° E	400	**105,3**	**0,4**	1990	Nydal et al. (1992)
Madrepora oculata Sample ID	Measurement ID	Latitude	Longitude	Depth (m)	**pMC**	**err pMC**	$Year_{lower\ limit}$ (37 yr)	$Year_{upper\ limit}$ (43 yr)
Mad 79	GifA 09467 – SacA 17521	67.5° N	9.4–9.5° E	300–350	**99.1**	**0.3**	1970	1964
Mad 75	GifA 09472 – SacA 17526	67.5° N	9.4–9.5° E	300–350	**104.1**	**0.3**	1974	1968
Mad 52	GifA 09481 – SacA 17535	67.5° N	9.4–9.5° E	300–350	**105.0**	**0.4**	1982	1978
Mad 32	GifA 09487 – SacA 17541	67.5° N	9.4–9.5° E	300–350	**105.2**	**0.3**	1992	1989
Mad 2	GifA 09496 – SacA 17673	67.5° N	9.4–9.5° E	300–350	**105.6**	**0.3**	2006	2006

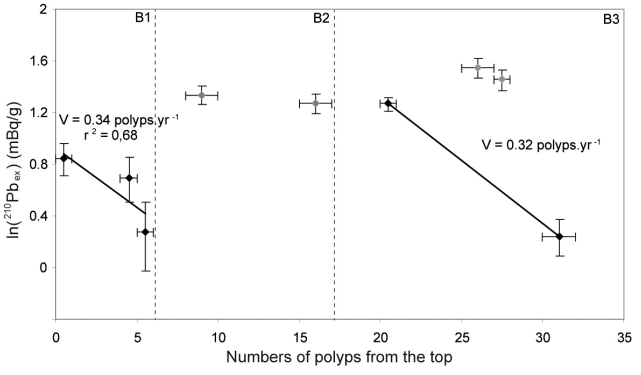

Fig. 9. ln-transformation of ^{210}Pb excess relative to the number of polyps from the top of the *Lophelia pertusa* specimen. Grey points presented high ^{228}Th activities and Mn content that were not included in the linear regression. The slope of these two linear regressions revealed a linear growth rate between 0.34 and 0.32 polyp yr^{-1} with a large uncertainty in relation to few points considered here. Horizontal dotted lines represent the limit of the three sampled branches (B1, B2, and B3).

coral genus appears presently (1) difficult to date by ^{210}Pb-^{226}Ra chronology and (2) less evident to provide a continuous record of environmental conditions.

6.3 Impact of metal oxide coatings and Mn corrections

As described in the result section, a correlation ($r^2 = 0.83$) is here present between Mn content and level of ^{210}Pb excess for the two older branch B2 and B3 of *L. pertusa* specimen (Fig. 5). The first growth rate estimation of *M. oculata* (2.58 ± 0.19 polyp yr^{-1}) was probably impacted by Mn contamination on the two oldest samples (Fig. 5). Thus, to overcome this influence a Mn correction for the radionuclides can be proposed. As a simple assumption, we estimate an additional ^{210}Pb contribution based on the measured $^{210}Pb_{ex}$/Mn ratio on *L. persuta* to correct the two older $^{210}Pb_{ex}$ values on *M. oculata*. This correction presumes that the ^{210}Pb excess associated to ^{210}Pb-^{226}Ra data would be negligible for the oldest parts of *L. pertusa* compared to $^{210}Pb_{oxide}$ and secondly the $^{210}Pb_{oxide}$/Mn ratio is presumed constant through time. Such a correction model brings back the two last samples to a Mn content equivalent to the other part of the *M. oculata* coral (blue area in Fig. 5) and allows us to correct these two $^{210}Pb_{ex}$ values from the $^{210}Pb_{oxide}$. Applying this simple model to the *M. oculata* specimen, which only at its base shows slightly elevated Mn concentrations yields an growth rate of 1.6 ± 0.3 polyp yr^{-1} and an age of 42–61 yr ($r^2 = 0.85$, $n = 7$). Thus the correction yields an increase of the coral age; however it is older than the estimated ^{14}C age of 40 yr. This indicates that the ^{210}Pb excess subtracted by the Mn correction is evidently too strong as based on the ^{14}C ages. However, for this correction we do not take into account the $^{210}Pb_{oxide}$ decay after its coating, which itself occurred between the basal age of the coral and the sampling date. Thus the $^{210}Pb_{oxide}$/Mn ratio must be lower than first estimated (Fig. 4), but without any information about the timing of the coating on each sample, we can not make a right correction, highlighting that an advanced cleaning procedure is a key issue to precisely date coral samples with ^{210}Pb-^{226}Ra method. However, even if the Mn correction remains uncertain due to the lack of information about the processes

and the period of formation of metal-enriched phases, the age estimation gives a minimum growth rate of this sample (1.6 ± 0.3 polyps yr^{-1}), while the first estimation without any correction gives a maximum growth rate of this *M. oculata* specimen (2.58 ± 0.19 polyps yr^{-1}). These results tend to confirm the ^{14}C estimation with a mean growth rate for this *M. oculata* about 2 polyps yr^{-1} and an age close to 40 yr.

This type of correction can not be applied on the *L. pertusa* specimen in relation to the very high Mn content of the two last branches (B2 and B3).

6.4 Coral growth rate comparison

For the *M. oculata* coral, only a few growth rate estimates are reported in the literature with values ranging from as low as 3 mm yr^{-1} to as high as 18 mm yr^{-1} with a maximum addition of 5 polyps yr^{-1}, obtained in aquaria (Orejas et al., 2008). The linear growth rate calculated for *M. oculata* is made on one single branch and therefore can not be simply compared to that obtained by Orejas et al. (2008), because in this study the numbers of polyps were not defined along one unique axis.

Overall, our growth rate estimates (around 2 polyps yr^{-1} or 11.2 cm yr^{-1}) best agree with the highest rates observed in aquaria and from in situ observations in the Nordic Seas. The northernmost reefs of *L. pertusa* and *M. oculata* are amongst the most active reefs known today, with sizes of individual colonies that exceed several meters of height and thus comprising thousands of individual coral generations.

Therefore, our present work brings new information about the maximum in situ linear growth rate and polyp regeneration rate of *M. oculata*. Our findings further highlight that a branching cold-water coral comprising several polyp generations, here 80, reflects the formation of aragonite skeleton over several decades, potentially allowing the reconstruction of physical and chemical properties of subsurface seawater at high latitude with a resolution of close to 1 yr.

Growth rate estimation of 26 ± 5 mm yr^{-1} for *L. pertusa* was made in the North Atlantic by measuring the size of colonies reported on oil and gas platforms over time (Bell and Smith, 1999; Gass and Roberts, 2006). Studies using stable isotopes estimated corallites growth of *L. pertusa* from 5 to 10 mm yr^{-1} (Mortensen and Rapp, 1998) and U-series measurements gave mean growth rates between 2.2 and 5.0 mm yr^{-1} (Pons-Branchu et al., 2005). Using coral fragments maintained in aquaria, Orejas et al. (2008) found extension rates of 15–17 mm yr^{-1} for *L. pertusa* while Brooke and Young (2009) with in situ experiments estimate this rate to 2–4 mm yr^{-1}. They explained these discrepancies between the documented linear growth rates for this species by the maturity difference of the polyps with a value >16 mm yr^{-1} and <5 mm yr^{-1} for new and more mature polyps, respectively. The *L. pertusa* investigated in this study seems to be characterized by a growth rate (0.33 polyps yr^{-1} or 8 mm yr^{-1}), in accordance with the range of previously reported data. These data should be taken with caution in relation to the high degree of growth rate uncertainty.

Therefore, we found that *M. oculata* was easier to work with than *L. pertusa* when providing continuous oceanographic archives to study hydrological changes with a yearly temporal resolution. However, *L. pertusa* may well be dated using a more rigorous cleaning and adopting a more complex sampling selection strategy based on the tangled growth of the successive poly generations.

7 Conclusions

^{210}Pb-^{226}Ra chronology was applied in this study for the first time to large branching specimens of *L. pertusa* and *M. oculata*, two constructional deep-sea scleractinian corals which form large deep-sea reefs that are of great ecological and conservation importance in the North Atlantic. ^{210}Pb and ^{226}Ra were not incorporated the same way into the deep-sea corals due to their different chemical behaviors in the aquatic environment. Pb isotopes readily scavenge onto particles, whereas Ra isotopes are soluble in seawater. To describe the temporal variation of ^{210}Pb, we had to take into account the decrease of ^{210}Pb initially incorporated to the skeleton ($^{210}Pb_{all}$) and, the ingrowth of ^{210}Pb from skeleton bound ^{226}Ra ($^{210}Pb_{rad}$). Since ^{226}Ra activities in both deep-sea corals were fairly constant, a constant uptake of ^{210}Pb with time was assumed and thus the ^{210}Pb-^{226}Ra chronology was applied to calculate the linear growth rate expressed in mm per year or polyp generation per year.

For the *M. oculata* colony, a linear growth rate was initially calculated at 2.6 ± 0.2 polyps yr^{-1} or 14.4 ± 1.1 mm yr^{-1} with an age of 31 yr obtained for the oldest corallite of this colonial deep-sea coral specimen. However, the relatively high Mn content for the oldest samples revealed a post-growth deposition of $^{210}Pb_{oxide}$ that induced an overestimation of the growth rate. A Mn correction was applied to these samples and a minimum growth rate was calculated at 1.6 ± 0.3 polyps yr^{-1}. But this simple correction does not take into account the $^{210}Pb_{oxide}$ decay after its coating and gives a minimum growth rate estimate. These results tend to confirm the ^{14}C estimation with a mean growth rate for this *M. oculata* about 2 polyps yr^{-1} and an age close to 40 yr old. Moreover, the age model indicates continuous growth of this *M. oculata* specimen during the entire period covered here. For the *L. pertusa*, Mn concentrations revealed a high level of contamination of metal/radionuclide-oxides especially for the oldest parts of the coral. For the upper branch of 15 cm a linear growth rate could be estimated at 0.33 polyps yr^{-1} or 8 mm yr^{-1}, but with large uncertainty. The presence of Mn-rich phases and the complexity of the *L. pertusa* growth, with frequent recruitment of coral polyps on older specimens, prevented accurate growth rate estimates for this important reef-forming species. In conclusion, the

^{210}Pb-^{226}Ra method applied to deep-sea corals can provide continuous, well-dated oceanographic archives over the last several decades with a less than 1 yr resolution to study intermediate or deep-seawater environmental parameters. But to further apply ^{210}Pb-^{226}Ra method to the major reef-building corals like *M. oculata* or *L. pertusa*, they need to be free of Mn/Fe coatings or an improved cleaning protocol has to be developed.

Acknowledgements. We would like to extend sincere thanks to the IFM-GEOMAR Jago submersible team together with crew and scientists aboard RV Polarstern during the Alfred Wegener Institute coordinated cruise ARK-XXII/1a. This work was supported by the CEA – CNRS and USVQ and first funded by the national project INSU/EVE/ICE-CTD. It was also partially funded by the EC-funded Framework 7 projects Knowledge-based Sustainable Management for Europe's Seas (KnowSeas grant agreement number 226675) and contributes to the European Project on Ocean Acidification (EPOCA grant agreement number 211384). This is LSCE contribution 4756. Thanks to the two anonymous reviewer for theirs constructive comments on the manuscript.

Edited by: J. Middelburg

The publication of this article is financed by CNRS-INSU.

References

Adkins, J. F., Cheng, H., Boyle, E. A., Druffel, E. R. M., and Edwards, R. L.: Deep-sea coral evidence for rapid change in ventilation of the deep North Atlantic 15,400 years ago, Science, 280, 725–728, 1998.

Adkins, J. F., Henderson, G. M., Wang, S.-L., O'Shea, S., and Mokadem, F.: Growth rates of the deep-sea scleractinia *Desmophyllum cristagalli* and *Enallopsammia rostrata*, Earth Planet. Sci. Lett., 227, 481–490, 2004.

Andrews, A. H., Cordes, E., Mahoney, M. M., Munk, K., Coale, K. H., Cailliet, G. M., and Heifetz, J.: Age and growth and radiometric age validation of a deep-sea, habitat-forming gorgonian (Primnoa resedaeformis) from the Gulf of Alaska, in: Biology of cold water corals, edited by: Watling, L. and Risk, M., Hydrobiologia, 471, 101–110, 2002.

Andrews, A. H., Stone, R. P., Lundstrom, C. C., and DeVogelaere, A. P.: Growth rate and age determination of bamboo corals from the northeastern Pacific Ocean using refined ^{210}Pb dating, Mar. Ecol-Pro. Ser., 397, 173–185, 2009.

Appleby, P. and Oldfield, F.: Uranium Series Disequilibrium, Application to Earth, Marine and Environmental Sciences, Chapter Application of Lead-210 to Sedimentation Studies Clarendon Press, Oxford, 731–778, 1992.

Arnold, M., Bard, E., Maurice, P., Valladas, H., and Duplessy, J.-C.: ^{14}C dating with the Gif-sur-Yvette Tandetron accelerator: status report and study of isotopic fractionation in the sputter ion source, Radiocarbon, 31, 284–291, 1989.

Baskaran, M., Hong, G.-H., Kim, S.-H., and Wardle, W. J.: Reconstructing seawater column ^{90}Sr based upon ^{210}Pb/^{226}Ra disequilibrium dating of mollusc shells, Appl. Geochem., 20, 1965–1973, 2005.

Bell, B. and Smith, J.: Coral growing on North Sea oil rigs, Nature, 402, 601, doi:10.1038/45127, 1999.

Berkman, P. A. and Ku, T.-L.: ^{226}Ra/Ba ratios for dating Holocene biogenic carbonates in the Southern Ocean: Preliminary evidences from Antarctic coastal mollusk shells, Chem. Geol., 144, 331–334, 1998.

Beuck, L., Vertino, A., Stepina, E., Karolczak, M., and Pfannkuche, O.: Skeletal response of *Lophelia pertusa* (Scleractinia) to bioeroding sponge infestation visualised with micro-computed tomography, Facies, 53, 157–176, 2007.

Broecker, W. S., Peng, T.-H., Ostlund, H. G., and Stuiver, M.: The Distribution of Bomb Radiocarbon in the Ocean, J. Geophys. Res., 90, 6925–6939, 1985.

Brooke, S. and Young, C. M.: In situ measurement of survival and growth of *Lophelia pertusa* in the northern Gulf of Mexico, Mar. Ecol.-Prog. Ser., 397, 153–161, 2009.

Cheng, H., Adkins, J. F., Edwards, R. L., and Boyle, E. A.: U-Th dating of deep-sea corals, Geochim. Cosmochimi. Ac., 64, 2401–2416, 2000.

Clark, M. R., Rowden, A. A., Schlacher, T., Williams, A., Consalvey, M., Stocks, K. I., Rogers, A. D., O'Hara, T. D., White, M., Shank, T. M., and Hall-Spencer, J. M.: The ecology of seamounts: structure, function and human impacts, Annu. Rev. Mar. Sci., 2, 253–278, 2010.

Cochran, J. K., Rye, D. M., and Landman, N. H.: Growth rate and habitat of Nautilus pompilius inferred from radioactive and stable isotope studies, Paleobiology, 7, 469–480, 1981.

Cochran, J. K., McKibbin-Vaughan, T., Dornblaser, M. M., Hirschberg, D., Livingston, H. D., and Buesseler, K. O.: ^{210}Pb scavenging in the North Atlantic and North Pacific Oceans, Earth Planet. Sci. Lett., 97, 332–352, 1990.

Colin, C., Frank, N., Copard, K., and Douville, E.: Neodymium isotopic composition of deep-sea corals from the NE Atlantic: implications for past hydrological changes during the Holocene, Quaternary Sci. Rev., 29, 2509–2517, 2010.

Copard, K., Colin, C., Douville, E., Freiwald, A., Gudmunsson, G., de Mol, B., and Frank, N.: Nd isotopes in deep-sea corals in the North-eastern Atlantic, Quaternary Sci. Rev., 29, 2499–2508, 2010.

Copard, K., Colin, C., Frank, N., Jeandel, C., Montero-Serrano, J.-C., Reverdin, G., and Ferron, B.: Nd isotopic composition of water masses and dilution of the Mediterranean outflow along the southwest European margin, Geochem. Geophys. Geosyst., 12, Q06020, doi:10.1029/2011GC003529, 2011.

Cottereau, E., Arnold, M., Moreau, C., Baqué, D., Bavay, D., Caffy, I., Comby, C., Dumoulin, J.-P., Hain, S., Perron, M., Salomon, J., and Setti, V.: Artemis, the new ^{14}C AMS at LMC14 in Saclay, France, Radiocarbon, 49, 291–299, 2007.

Dodge, R. E. and Thomson, J.: The natural radiochemical and growth records in contemporary hermatypic corals from the Atlantic and Caribbean, Earth Planet. Sci. Lett., 23, 313–322, 1974.

Druffel, E. R. M., King, L. L., Belastock, R. A., and Buesseler, K. O.: Growth rate of a deepsea coral using ^{210}Pb and other isotopes, Geochim. Cosmochim. Ac., 54, 1493–1500, 1990.

Fairbanks, R. G. and Dodge, R. E.: Annual periodicity of the 18O/16O and 13C/12C ratios in the coral Montastrea annularis, Geochim. Cosmochim. Ac., 43, 1009–1020, 1979.

Fenton, G. E., Short, S. A., and Ritz, D. A.: Age determination of orange roughy, Hoplostethus atlanticus (Pisces: Trachichthyidae) using ^{210}Pb:^{226}Ra disequilibria, Mar. Biol., 109, 197–202, 1991.

Flynn, W. W.: The determination of low levels of polonium-210 in environmental samples, Anal. Chim. Acta, 43, 221–227, 1968.

Fosså, J. H., Lindberg, B., Christensen, O., Lundalv, T., Svellingen, I., Mortensen, P., and Alvsvag, J.: Mapping of Lophelia reefs in Norway: experiences and survey methods, in: Cold-water Corals and Ecosystems, edited by: Freiwald, A. and Roberts, J. M., 337–370, Berlin – Heidelberg, Germany, Springer-Verlag, 2005.

Frank, N., Paterne, M., Ayliffe, L., van Weering, T., Henriet, J. P., and Blamart, D.: Eastern North Atlantic deep-sea corals: tracing upper intermediate water Δ^{14}C during the Holocene, Earth Planet. Sci. Lett., 219, 297–309, 2004.

Frank, N., Lutringer, A., Paterne, M., Blamart, D., Henriet, J. P, Van Rooij, D., and Van Werinng, T.: Deepwater corals of the northeastern Atlantic margin : carbonate mound evolution and upper intermediate water ventilation water ventilation during the Holocene, in: Cold water Corals and Ecosystems, edited by: Freiwald, A. and Roberts, J. M., 113–133, Berlin, Heidelberg, Germany, Springer-Verlag, 2005.

Frank, N., Ricard, E., Lutringer-Paquet, A., van der Land, C., Colin, C., Blamart, D., Foubert, A., Van Rooij, D., Henriet, J. P., de Haas, H., and van Weering, T.: The Holocene occurrence of cold water corals in the NE Atlantic: Implications for coral carbonate mound evolution, Mar. Geol., 266, 129–142, 2009.

Frank, N., Freiwald, A., López Correa, M., Wienberg, C., Eisele, M., Hebbeln, D., Van Rooij, D., Henriet, J. P., Colin, C., van Weering, T., de Haas, H., Buhl-Mortensen, P., Roberts, J. M., De Mol, B., Douville, E., Blamart, D., and Hatte, C.: Northeastern Atlantic cold-water coral reefs and climate, Geology, 39, 743–746, 2011.

Gass, S. E. and Roberts, M.: The occurrence of the cold-water coral *Lophelia pertusa* (Scleractinian) on oil and gas plateforms in the North Sea: Colony growth, recruitment and environmental controls on distribution, Mar. Pollut. Bull., 52, 549–559, 2006.

Golberg, E.: Geochronology with Lead-210, chapter Radioactive Dating, IAEA Pan. P., 121–131, 1963.

Grigg, R. W.: Growth rings: annual periodicity in two gorgonian coral, Ecology, 55, 876–881, 1974.

Guinotte, J. M., Orr, J., Cairns, S., Freiwald, A., Morgan, L., and George, R.: Will human-induced changes in seawater chemistry alter the distribution of deep-sea scleractinian corals?, Front. Ecol. Env., 4, 141–146, 2006.

Hall-Spencer, J. M., Tasker, M., Soffker, M., Christiansen, S., Rogers, S., Campbell, M., and Hoydal, K.: The design of Marine Protected Areas on High Seas and territorial waters of Rockall, Mar. Ecol-Prog. Ser., 397, 305–308, 2009.

Heikoop, J. M., Hickmott, D. D., Risk, M. J., Shearer, C. K., and Atudorei, V.: Potential climate signal from the deep-sea gorgonian coral Primnoa resedaeformis, Hydrobiology, 471, 117–124, 2002.

Krishnaswami, S. and Cochran, J. K.: Radioactivity in the Environment, in: U–Th Series Nuclides in Aquatic Systems, 13, Elsevier, New York, 458 pp., 2008.

Lomitschka, M. and Mangini, A.: Precise Th/U-dating of small and heavily coated samples of deep sea corals, Earth Planet. Sci. Lett., 170, 391–401, 1999.

Maier, C., Hegeman, J., Weinbauer, M. G., and Gattuso, J.-P.: Calcification of the cold-water coral Lophelia pertusa, under ambient and reduced pH, Biogeosciences, 6, 1671–1680, doi:10.5194/bg-6-1671-2009, 2009.

Mangini, A., Lomitschka, M., Eichstädter, R., Frank, N., Vogler, S., Bonani, G., Hajdas, I., and Pätzold, J.: Coral provides way to age deep water, Nature, 392, 347, doi:10.1038/32804, 1998.

Moore, W. S. and Krishnaswami, S.: Coral growth rates using Ra-228 and Pb-210, Earth Planet. Sci. Lett., 15, 187–190, 1972.

Mortensen, P. B. and Rapp, H. T.: Oxygen and carbon isotope ratios related to growth line patterns in skeletons of *Lophelia pertusa* (L) (Anthozoa: Scleractinia): implications for determination of linear extension rates, Sarsia, 83, 433–446, 1998.

Nydal, R., Gislefoss, J., Skjelvan, I., Skogseth, F., Jull, A. J. T., and Donahue, D. J.: ^{14}C profiles in the Norwegian and Greenland Seas by conventional and AMS measurements, Radiocarbon, 34, 717–726, 1992.

Orejas, C., Gori, A., and Gili, J. M.: Growth rates of live *Lophelia pertusa* and *Madrepora oculata* from the Mediterranean Sea maintained in aquaria, Coral Reefs, 27, 255, doi:10.1007/s00338-007-0350-7, 2008.

Ostlund, H. G., Dorsey, H. G., and Rooth, C. G.: GEOSECS North Atlantic radiocarbon and tritium results, Earth Planet. Sci. Lett., 23, 69–86, 1974.

Pons-Branchu, E., Hillaire-Marcel, C., Deschamps, P., Ghaleb, B., and Sinclair, D. J.: Early diagenesis impact on precise U-series dating of deep-sea corals: Example of a 100-200-year old Lophelia pertusa sample from the northeast Atlantic, Geochimi. Cosmochim. Ac., 69, 4865–4879, 2005.

Reyss, J.-L., Schmidt, S., Legeleux, F., and Bonté, P.: Large, low background well-type detectors for measurements of environmental radioactivity, Nucl. Instrum. Meth. A, 357, 391–397, 1995.

Risk, M., Hall-Spencer, J. M., and Williams, B.: Climate records from the Faroe-Shetland Channel using *Lophelia pertusa* Linnaeus, 1758 in: Cold water Corals and Ecosystems, edited by: Freiwald, A. and Roberts, J. M., Berlin, Heidelberg, Germany, Springer-Verlag, 2005.

Roberts, J. M., Wheeler, A., Friewald, A., and Cairns, S.: Cold-water corals the biology and geology of deep-sea coral habitats, Cambridge University Press, 334 pp., 2009.

Rodolfo-Metalpa, R., Houlbrèque, F., Tambutté, E., Boisson, F., Baggini, C., Patti, F. P., Jeffree, R., Fine, M., Foggo, A., Gattuso, J.-P., and Hall-Spencer, J. M.: Coral and mollusc resistance to ocean acidification adversely affected by warming, Nature Climate Change, 1, 308–312, 2011.

Rüggeberg, A., Fietzke, J., Liebetrau, V., Eisenhauer, A., Dullo, W.-C., and Freiwald, A.: Stable strontium isotopes (d88/86Sr) in cold-water corals – a new proxy for reconstruction of intermediate ocean water temperatures, Earth Planet. Sci. Lett., 269, 570–575, 2008.

Schmidt, S. and Cochran, J. K.: Radium and radium-daughter nuclides in carbonates: a briefs overview of strategies for determin-

ing chronologies, J. Environ. Radioactiv., 101, 530–537, 2010.

Schuller, D., Kadko, D., and Smith, C. R.: Use of ^{210}Pb/^{226}Ra disequilibria in the dating of deep-sea whale falls, Earth Planet. Sci. Lett., 218, 277–289, 2004.

Sherwood, O. A., Edinger, E. N., Guilderson, T. P., Ghaleb, B., Risk, M. J., and Scott, D. B.: Late Holocene radiocarbon variability in Northwest Atlantic slope waters, Earth Planet. Sci. Lett., 275, 146–153, 2008.

Söffker, M., Sloman, K. A., and Hall-Spencer, J. M.: in situ observations of fish associated with coral reefs off Ireland, Deep-Sea Res. Pt. 1, 58, 818–825. 2011.

Stuiver, M. and Polach, H. A.: Discussion reporting of ^{14}C data, Radiocarbon, 19, 355–363, 1977.

Thresher, R., Rintoul, S. R., Koslow, C., Weidman, C., Adkins, J., and Proctor, C.: Oceanic evidence of climate change in Southern Australia over the last three centuries, Geophys. Res. Lett., 31, LO7212, doi:10.1029/2003GL018869, 2004.

Tisnérat-Laborde, N., Poupeau, J.-J., Tannau, J.-F., and Paterne, M.: Development of a semi-automated system for routine preparation of carbonate sample, Radiocarbon, 43, 299–304, 2001.

Tittensor, D. P., Baco, A. R., Hall-Spencer, J. M., Orr, J. C., and Rogers, A. D.: Seamounts as refugia from ocean acidification for cold-water stony corals, Mar. Ecol., 31, 212–225, 2010.

Turekian, K. K. and Cochran, J. K.: Flow rates and reaction rates in the Galapagos Rise spreading center hydrothermal system as inferred from ^{228}Ra/^{226}Ra in vesicomyid clam shells, Proc. Natl. Acad. Sci. USA., 83, 6241–6244, 1986.

van Beek, P. and Reyss, J. L.: ^{226}Ra in marine barite: new constraints on supported ^{226}Ra, Earth Planet. Sci. Lett., 33, 147–161, 2001.

van de Flierdt, T., Robinson, L. F., Adkins, J. F., Hemming, S. R., and Goldstein, S. L.: Temporal stability of the neodymium isotope signature of the Holocene to glacial North Atlantic, Paleoceanography, 21, 1–6, 2006.